JOBIMB, 2026, Vol 14, No 1, 28-36
https://doi.org/10.54987/jobimb.v14i1.822

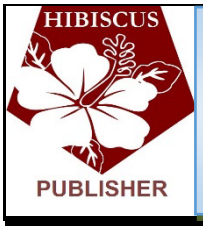

JOURNAL OF BIOCHEMISTRY, MICROBIOLOGY AND BIOTECHNOLOGY
Website: http://journal.hibiscuspublisher.com/index.php/JOBIMB/index

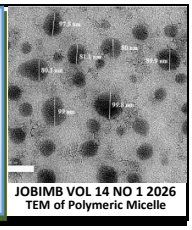

Kojic Monooleate Loaded Nanostructured Lipid Carriers (NLCs) for Enhanced Sunscreen Formulation: Optimisation via Response Surface Methodology

Nur Farah Syazwahazwani Sufatan[1,2], Siti Efliza Ashari[1,2,3]*

[1]Department of Chemistry, Faculty of Science, Universiti Putra Malaysia, 43400 UPM, Serdang, Selangor, Malaysia.
[2]Bioprocessing & Biomanufacturing Research Group, University Driven Research Group, Universiti Putra Malaysia, 43400 UPM, Serdang, Selangor Malaysia.
[3]Centre for Foundation Studies in Sciences, Universiti Putra Malaysia, 43400 UPM, Serdang, Selangor, Malaysia.

*Corresponding author:
Siti Efliza Ashari
Centre for Foundation Studies in Sciences,
Universiti Putra
Malaysia, 43400 UPM,
Serdang, Selangor,
Malaysia.
Email: ctefliza@upm.edu.my

History

Received: 20th April 2026
Received in revised form: 21st June 2026
Accepted: 30th July 2026

Keywords

Nanostructured lipid carriers
Kojic monooleate
Sunscreen formulation
Tyrosinase inhibition
Response Surface Methodology

SDG Keywords

SDG 3 Good health and well-being
SDG 9 Industry, innovation and infrastructure
SDG 12 Responsible consumption and production

Abstract

Nanostructured lipid carriers (NLCs) are promising topical delivery systems for improving the dispersion and formulation performance of lipophilic cosmeceutical actives. Chronic ultraviolet (UV) exposure contributes to photoageing and hyperpigmentation, creating a demand for multifunctional sunscreen formulations that provide photoprotection together with tyrosinase inhibition. This study aimed to formulate and optimise a kojic monooleate (KMO)-containing NLC sunscreen using sun protection factor (SPF) as the primary optimisation response. KMO was incorporated as a tyrosinase-inhibitory active together with titanium dioxide, zinc oxide and avobenzone as UV filters. NLCs were prepared by bath ultrasonication followed by high-shear homogenisation, and a D-optimal response surface methodology was applied to optimise the formulation. Analysis of variance demonstrated that the quadratic model was significant ($F = 196.33$, $p < 0.05$) with a non-significant lack of fit, indicating good model predictability. The optimised formulation achieved an in vitro SPF of 38.88, a mean particle size of 170.10 nm, a polydispersity index of 0.326 and a pH of 4.88. No visible phase separation was observed after centrifugation, whereas freeze–thaw cycling increased particle size and polydispersity index, indicating reduced colloidal stability under thermal stress. The optimised formulation also exhibited acceptable spreadability and 78.08% mushroom tyrosinase inhibition at 250 µg/mL. These findings provide preliminary evidence supporting the potential of KMO-containing NLCs as SPF-oriented multifunctional sunscreen formulations. However, further evaluation of UVA protection, critical wavelength, photostability, comprehensive nanoparticle characterisation and cell-based melanogenesis is required before broad-spectrum photoprotection and biological depigmenting efficacy can be established.

INTRODUCTION

Excessive exposure of human skin to UV radiation poses a risk to human skin as it results in sunburn, photoageing and increases the risk of skin cancer. The cosmetics manufacturers have also focused on creating superior broad-spectrum sunscreens that are effective in blocking UVA (320-400 nm) and UVB (290-320 nm) radiation. Although organic and inorganic UV filters have improved, some of the drawbacks of traditional sunscreen products include poor stability, low efficacy, and even possible irritation of the skin by chemical filters [1,2]. Additionally, there has been a significant rise in the global demand in effective sunscreen formulations not just due to the increased awareness about skin cancer prevention but also owing to the increasing cosmeceutical market that has stressed multifunctional skin protection and cosmeceutical advantages. Due to the growth in global skin health awareness, the sunscreen market is expected to reach USD 38.6 billion by 2035, as a result of increasing consumer interest in multifunctional products with both UV protection and antioxidant, anti-ageing, and depigmenting properties [3].

In recent years, nanotechnology is being embraced as a promising approach to overcome these challenges. Among various nano-based delivery systems, nanostructured lipid carriers (NLCs) have gained significant interest as a novel strategy for enhancing the performance of topical formulations. NLCs, the second generation of lipid nanoparticles, are composed of a blend of solid and liquid lipids that allow for improved drug loading, controlled release, and enhanced chemical stability [2,4]. NLCs have also shown to be more physicochemically stable, more able to encapsulate drugs, and more reproducible in drug release profile on storage compared to solid lipid nanoparticles (SLNs) [5]. In addition to their great encapsulation efficiency, NLCs increase stability of UV filters and prevent skin irritation through encapsulation of the filters and minimisation of direct contact between the filters and the skin. NLCs possess better cosmetic properties, such as an improved skin feel and reduced white cast compared with traditional emulsions [6]. These properties allow NLCs to be highly applicable in delivering lipophilic active ingredients in sunscreen formulations.

Titanium dioxide (TiO_2) and zinc oxide (ZnO) nanoparticles are widely investigated as inorganic UV filters because of their ability to attenuate ultraviolet radiation while reducing the opaque appearance associated with larger particles. Despite these advantages, their dermal penetration and potential toxicity remain important safety considerations in sunscreen development. A safety review by the Australian Therapeutic Goods Administration reported that most in vitro and in vivo studies demonstrated no or minimal penetration of TiO_2 and ZnO nanoparticles beyond the stratum corneum, suggesting a low likelihood of systemic exposure when sunscreen products are used as directed [7]. However, nanoparticle safety may depend on factors such as primary particle size, aggregation state, surface coating, crystalline form, concentration, and formulation characteristics.

Kojic monooleate (KMO), a kojic acid and oleic acid derivative, a stable ester, is a potential multifunctional product in sunscreen applications. KMO is a derivative of a fungal metabolite and is a tyrosinase inhibitor that has been used to treat hyperpigmentation disorders [8]. KMO is more stable thermally and photostable compared to kojic acid and can tolerate pH changes between 4 and 9 and thus is more useful in cosmetic applications [9]. Furthermore, integration of KMO into a sunscreen formula must not only inhibit skin damage due to UV but also to regulate melanin production, thus repairing the appearance of hyperpigmentation and uneven skin tone sunspots and skin colour imperfections. [9]. Formulation and processing parameters have to be optimised to achieve the appropriate particle size and stability to develop NLC-based sunscreen formulations. RSM offers a systematic way of assessing factor impact and interaction with fewer experiments [10]. This method enhances the formulation process by enabling the identification of optimal conditions in a cost-effective and time-efficient manner. In this study, RSM was employed to optimise four key formulation parameters percentage of titanium dioxide, zinc oxide, avobenzone, and olive oil with sun protection factor (SPF) value as the response. In addition, the potential of the optimised KMO-loaded NLC sunscreen was evaluated through a tyrosinase inhibition assay to assess its efficacy in reducing melanin production. To date, limited studies have systematically optimised KMO-loaded NLC formulations for multifunctional sunscreen applications integrating ultraviolet protection with tyrosinase-inhibitory activity.

Therefore, this study aimed to develop and optimise a KMO-loaded NLC sunscreen formulation using response surface methodology. The percentages of titanium dioxide, zinc oxide, avobenzone, and olive oil were investigated as formulation variables, with SPF selected as the primary optimisation response. The optimised formulation was subsequently evaluated for its physicochemical characteristics, physical stability, spreadability, and in vitro tyrosinase-inhibitory activity to determine its potential as a multifunctional cosmeceutical formulation.

SPF was selected as an erythema-weighted response for screening and optimising the effects of the investigated formulation variables. However, SPF predominantly reflects protection against UVB-induced erythema and may not fully represent the UVA contribution of avobenzone. Accordingly, the developed model should be interpreted as an SPF-oriented optimisation model and not as a comprehensive evaluation of UVA or broad-spectrum protection. No broad-spectrum claim is therefore made in the present study. A complete assessment of sunscreen performance would require additional determination of UVA protection, including UVA protection factor and critical wavelength, using an appropriate standardised method such as ISO 24443:2021 [11]. Under United States Food and Drug Administration requirements, a mean critical wavelength of at least 370 nm is required for classification as a broad-spectrum sunscreen [12]. Further evaluation of UVA protection, photostability, and water resistance is therefore required before broad-spectrum performance claims can be established.

MATERIALS AND METHODS

Materials

Kojic monooleate (KMO) was synthesised according to the established method reported by Jumbri et al. [13]. Compritol 888 ATO was used as the solid lipid, while olive oil was used as the liquid lipid. Tocopherol was incorporated as an antioxidant. Tween 80 was used as surfactant. The UV filters used in this study were titanium dioxide, zinc oxide, and avobenzone. Phenoxyethanol was used as a preservative, while xanthan gum and sodium hyaluronate were used as gelling agents. Fragrance was added as a cosmetic additive. Mushroom tyrosinase from Agaricus bisporus and L-tyrosine were used for the tyrosinase inhibition assay. Unless otherwise stated, all chemicals and materials were obtained from Sigma-Aldrich and were of analytical or cosmetic grade.

Formulation of NLC

The NLC was prepared using a combination of bath ultrasonication (Power Sonic 405, Korea) and high shear homogenisation (T25 digital, IKA-Werk, Germany) techniques. Compritol 888 ATO was used as the solid lipid, while KMO, olive oil, and tocopherol as the liquid lipid phase. The lipid phase was heated to 5–10 °C above the melting point of the solid lipid. The aqueous phase, containing distilled water, Tween 80, aloe vera extract, allantoin, sodium hyaluronate, and xanthan gum, was prepared separately. Both phases were heated to 85 °C under continuous magnetic stirring until homogeneous. The aqueous and lipid phases were then combined and stirred for 15 minutes. Titanium dioxide, zinc oxide, and avobenzone were added to the dispersion, which was subsequently subjected to bath ultrasonication at room temperature for 15 minutes. The sonicated dispersion was homogenised at 9000 rpm for 10 minutes. Finally, phenoxyethanol and fragrance were added, and the formulation was further homogenised for 1 minute.

Optimisation of nanostructured lipid carriers (NLC) formulation using RSM

Experimental design and statistical analysis

D-optimal response surface design prioritises compositional balance for efficacy and stability of the mixture. In this study, the D-optimal design was implemented to evaluate the effects of four key formulation components (titanium dioxide (A), zinc oxide (B), avobenzone (C), and olive oil (D)) on the SPF of the NLC-based sunscreen as the response. 18 randomised formulations were generated using Design Expert software (v13.0, Stat-Ease Inc., USA) under a quadratic polynomial model to capture linear, interaction, and quadratic effects. A quadratic polynomial model was fitted, and ANOVA was performed to determine model significance. **Table 1** summarises limitations on proportions of the formulation components. All compositions are expressed as percentage weight by weight (% w/w). Purified water was added in a quantity sufficient to obtain a final formulation weight of 30 g. The other ingredients concentration is presented in **Table 2**.

Table 1. Constraint of independent variables proportions.

Independent Variables	Goal	Lower Limit	Upper Limit
A: Titanium dioxide (%)	In range	2	5
B: Zinc Oxide (%)	In range	5	10
C: Avobenzone (%)	In range	2	3
D: Olive oil (%)	In range	1	4

Table 2. Fixed formulation components and concentrations.

Ingredients	Function	Concentration (% w/w)
Compritol 888 ATO	Solid lipid	6.0
Kojic monooleate (KMO)	Active ingredients	6.0
Tween 80	Surfactant/emulsifier	1.0
Tocopherol	Antioxidant	3.0
Aloe vera extract	Emollient	3.0
Allantoin	Emollient	0.8
Sodium hyaluronate	Humectant agent	0.5
Xanthan gum	Thickening agent	0.5
Phenoxyethanol	Preservative	1.0
Fragrance	Fragrance	0.7
Distilled water	Continuous phase	q.s.to 30 g

The experimental SPF values were fitted to a second-order polynomial regression model and ANOVA was performed to assess the model's statistical significance and the influence of individual factors and quadratic terms interactions:

$$Y = \beta_0 + \beta_1X_1 + \beta_2X_2 + \beta_3X_3 + \beta_4X_4 + \beta_{11}X_1^2 + \beta_{22}X_2^2 + \beta_{33}X_3^2 + \beta_{44}X_4^2 + \beta_{12}X_1X_2 + \beta_{13}X_1X_3 + \beta_{14}X_1X_4 + \beta_{23}X_2X_3 + \beta_{24}X_2X_4 + \beta_{34}X_3X_4$$

where Y represents the predicted SPF value; β_0 is the intercept; β_1, β_2, β_3, and β_4 are the linear coefficients; β_{11}, β_{22}, β_{33}, and β_{44} are the quadratic coefficients; and β_{12}, β_{13}, β_{14}, β_{23}, β_{24}, and β_{34} represent the interaction coefficients between the independent variables.

Model verification

The effectiveness of the predicted response values was assessed by validating the final model. To validate the model, three formulations with different component ratios were selected and tested. Predicted SPF values were compared with experimental results using residual standard error (RSE) using equation 1:

$$\text{RSE}(\%) = \frac{\text{Experimental value} - \text{Predicted value}}{\text{Predicted value}} \times 100\% \qquad \text{Eqn. 1}$$

Physicochemical characterisation of nanostructured lipid carriers (NLC) formulation

Particle size analysis

The hydrodynamic particle size and polydispersity index (PDI) of the NLC formulations were determined by dynamic light scattering using a Zetasizer Nano ZS (Malvern Instruments Ltd., Malvern, UK), based on the general DLS principles described in ISO 22412:2025 [14] and by Stetefeld et al. [15]. Before analysis, 10 µL of each NLC dispersion was diluted with deionised water to a final volume of 1.0 mL, corresponding to a 1:100 (v/v) dilution. The diluted samples were subjected to bath sonication for 15 minutes and equilibrated at 25 °C before measurement. Measurements were performed at a backscatter detection angle of 173°. Particle size was reported as the intensity-weighted Z-average hydrodynamic diameter, while the PDI was obtained using cumulants analysis. Three measurements were conducted for each formulation, and the results were expressed as mean ± standard deviation.

Stability study

Centrifugation and freeze thaw cycling were used to determine the physical stability of the optimised version of NLC formulation and visible phase separation was considered as the main indicator of instability. In the centrifugation assay, three duplicate samples were centrifuged at 4000 rpm and 15 minutes and then checked to observe the separation of the phases. To achieve freeze thaw stability, the formulation was exposed to three freeze thaw cycles. Cycles were performed by freezing at −18 °C for 22 hours and then thawing at 40 °C at a water bath 2 hours. The cycle was repeated over three consecutive days and the samples were observed to show any evidence of instability [16].

Organoleptic analysis & spreadability

The organoleptic evaluation was performed to determine the appearance, colour, odour, and texture of the formulation. Variations in these parameters were observed visually as a sign of the quality of raw materials and possible instability of the formulation during storage. Spreadability, an important quality parameter influencing performance of topical formulations was evaluated using the parallel-plate glass method described by Varma et al. with modification [17,18]. To evaluate mechanical spreading behaviour, the formulation (1 g) was confined between two identically dimensioned glass plates and a static load of 100 g weight was imposed on the upper plate for 60 seconds. The spread diameters were recorded in triplicate, and corresponding spreadability values were derived using the following equation 2:

$$s = \frac{m \times l}{t} \times 100\% \qquad \text{Eqn. 2}$$

where, s is spreadability, m is weight place on top of glass slide, l is length of the upper slide, and t is time taken.

SPF value

SPF was determined using the method described by Qian et al. [19]. Sample analysis was performed utilizing a UV spectrometer. SPF analysis was conducted with a 2600 UV–VIS spectrophotometer. Prior to the test, 2 mg/cm² of cream was uniformly applied onto a quartz slide and allowed to dry for 20 minutes.

The SPF value was determined by calculating the absorbance values within the wavelength range of 290–400 nm, with 5 nm wavelength increments. SPF values can be obtained from equation 3:

$$SPF\ Value = \frac{\sum_{290}^{400} E_\lambda S_\lambda}{\sum_{290}^{400} E_\lambda S_\lambda T_\lambda} \quad \text{Eqn. 3}$$

where E_λ = erythemal effect spectrum, S_λ = solar spectral irradiance and T_λ = spectral transmittance of the sample. The erythema efficiency at each wavelength was determined in terms of relative units according to the Commission Internationale de l′ Eclairage (CIE) and the International Organisation for Standardisation (ISO), using the following formula (ISO, 1999):

E_λ = 1.0 for wavelengths 250nm ≤ l ≤ 298nm
E_λ = 100.094(298-λ) for 298 < λ ≤ 328nm

Tyrosinase inhibition study

The tyrosinase inhibition activity of KMO, KMO-loaded NLC, and kojic acid was evaluated based on a modified method by Roselan et al. [20]. Kojic acid served as positive control due to its well-established depigmenting effect. Briefly, mushroom tyrosinase (Agaricus bisporus) was dissolved in 50 mM phosphate-buffered saline (PBS) to a concentration of 1000 U/mL. The samples were prepared via serial dilution to obtain final concentrations of 5, 10, 25, 50, 100, 250, and 500 µg/mL. In each well of a 96-well plate, 50 µL of test sample was combined with 260 µL of L-tyrosine substrate and pre-incubated for 2 minutes at 25 °C prior to initiate the enzymatic reaction. Then 50 µL of the enzyme solution was added and the plate was incubated for 10 minutes. Blank samples were made by substituting the sample with 50 µL of PBS. Enzymatic activity was determined by measuring absorbance at 492 nm with an ELISA micro plate reader. All assays were performed in triplicate. For the control, the sample was replaced with 50 µL of PBS. The tyrosinase inhibitory activity was calculated as in equation 4:

$$SPF\ Value = \frac{\sum_{290}^{400} E_\lambda S_\lambda}{\sum_{290}^{400} E_\lambda S_\lambda T_\lambda} \quad \text{Eqn. 4}$$

where A and B are the absorbance of the control and the sample, respectively.

Data are presented as mean ± standard deviation (SD) from three replicate measurements. Tyrosinase-inhibitory activity was analysed using two-way analysis of variance (ANOVA), with formulation type and concentration as the independent factors, followed by Tukey's multiple-comparisons test. Differences were considered statistically significant at $p < 0.05$

RESULTS AND DISCUSSION

Model fitting and ANOVA analysis

ANOVA indicates the model was significant ($p < 0.001$) with a high R-squared value ($R^2 = 0.9989$), confirming model adequacy. SPF was most influenced by titanium dioxide, followed by zinc oxide and avobenzone. Olive oil had a minor effect.

Optimisation predicted an SPF of 39.09, and the experimental value of 38.88 showed good agreement (RSE < 5%). The mean of SPF value of NLC sunscreen obtained experimentally, according to the Design of Experiments (DOE), is tabulated in **Table 3**.

Table 3. The mean of SPF value of NLC sunscreen.

Run	A (%)	B (%)	C (%)	D (%)	SPF Value	
					Experimental Value	Predicted Value
1	4.2	10.0	2.0	4.0	28.01	28.29
2	3.2	8.0	2.6	1.0	21.06	20.91
3	2.0	5.0	2.0	1.0	5.57	5.88
4	2.0	10.0	2.8	4.0	17.81	18.04
5	2.0	5.4	3.0	4.0	13.87	13.93
6	4.2	10.0	3.0	1.8	29.18	29.59
7	4.0	6.8	2.0	2.0	16.80	17.27
8	3.2	5.0	2.6	2.8	16.64	16.43
9	5.0	5.0	3.0	1.0	36.06	35.99
10	4.4	10.0	3.0	4.0	30.05	29.39
11	2.0	6.6	2.0	4.0	15.40	15.22
12	5.0	10.0	2.0	1.0	37.78	37.66
13	5.0	5.0	2.0	4.0	31.16	31.08
14	2.0	10.0	2.0	2.0	17.18	17.03
15	2.0	6.2	3.0	1.8	13.23	13.04
16	4.2	6.2	3.0	4.0	24.97	25.32
17	4.0	6.8	2.0	2.0	17.79	17.27
18	5.0	8.0	2.6	2.8	38.88	39.09

Note: A: Titanium dioxide concentration, B: Zinc Oxide concentration- C: Avobenzone concentration- D: Olive oil concentration. All % are in (w/w) %.

The close agreement between actual and predicted SPF values indicates that the fitted model adequately represented the experimental data within the studied design space. The final equation to predict the SPF value in terms of coded factors for the second-order polynomial is shown in equation 5:

$$Y = 20.71+10.60A + 3.47B + 1.65C + 0.5437D + 0.3544AB + 1.14AC -0.2715AD -1.32BC -1.38BD -1.58CD +6.67A2 + 0.1783B2 -3.66C2 +1.29D2. \quad \text{Eqn. 5}$$

Where A, B, C and D represent the values of titanium dioxide, zinc oxide, avobenzone and olive oil, respectively. The predicted SPF values derived from the model versus the actual SPF values obtained from the experimental data shows that the model was successful in capturing the correlation between all the independent variables, with R2=0.9989 as shown in **Fig. 1.**

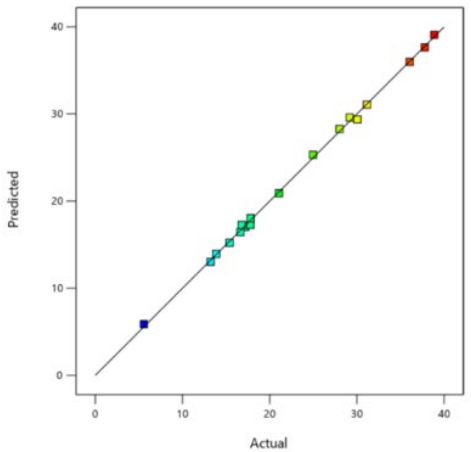

Fig. 1. Scatter plot of predicted SPF values versus actual SPF values from four-factor D- Optimal Design.

ANOVA results for the effects of all independent variables were implemented using Design-Expert (version 13; Stat-Ease Inc., Minneapolis, MN, USA) to investigate the suitability and the significance of the final model (**Table 4)**.

Table 4. ANOVA results for the effect of all independent variables.

Source	Sum of Squares	df	Mean Square	F-value	p-value
Model	1533.59	14	109.54	196.33	0.0005
A-Titanium Dioxide	1023.34	1	1023.34	1834.14	<0.0001
B-Zinc oxide	115.81	1	115.81	207.57	0.0007
C-Avobenzone	33.25	1	33.25	59.60	0.0045
D-Olive oil	2.72	1	2.72	4.88	0.1142
AB	0.8127	1	0.81	1.46	0.3134
AC	10.32	1	10.32	18.49	0.0231
AD	0.4655	1	0.47	0.83	0.4284
BC	14.39	1	14.39	25.80	0.0147
BD	12.69	1	12.69	22.74	0.0175
CD	20.63	1	20.63	36.98	0.0089
A^2	103.20	1	103.20	184.97	0.0009
B^2	0.0775	1	0.0775	0.14	0.7341
C^2	27.56	1	27.56	49.39	0.0059
D^2	4.03	1	4.03	7.22	0.0747
Residual	1.67	3	0.5579		
Lack of Fit	1.18	2	0.5919	1.2078	0.5410
Pure Error	0.4900	1	0.4900		
Cor Total	1535.26	17			

The statistical analysis confirmed the significance of the quadratic model, as indicated by a high Model F-value of 196.33 and a corresponding p-value of 0.0005. These results suggest that the model's predictive performance is unlikely to be due to random error. Importantly, the lack-of-fit was not significant, demonstrating that the model appropriately describes the variation in SPF values within the tested design space. Among the studied variables, titanium dioxide (A) showed the strongest influence on SPF, followed by zinc oxide (B) and avobenzone (C), while olive oil showed a comparatively minor effect.

The model's reliability was further supported by a predicted R^2 value of 0.8655 and an adjusted R^2 of 0.9938, indicating both strong predictive accuracy and consistency with the observed data. Additionally, the Adequate Precision ratio used to evaluate signal-to-noise was 48.71, well above the threshold of 4. This confirms that the model provides an adequate signal and is suitable for navigating the formulation design space. The model summary statistics are presented in **Table 5**.

Table 5. Regression coefficient results for the final model.

Std. Dev.	0.7470	R^2	0.9989
Mean	22.86	Adjusted R^2	0.9938
C.V. %	3.27	Predicted R^2	0.8655
		Adeq Precision	48.7106

Response surface analysis

The main consideration of this study is to obtain maximum SPF value. Three-dimensional (3D) response surface is a graphical representation of the regression function. It is used to show how independent variables affected the response variables (SPF value).

Effect of titanium dioxide and zinc oxide

Fig. 2(a) illustrates the combined effect of titanium dioxide (A) and zinc oxide (B), with avobenzone (C) and olive oil (D) held constant. SPF increased as the concentration of titanium dioxide rose from 2% to 5% (w/w), consistent with previous findings [21,22].

This enhancement is attributed to titanium dioxide's strong UV-blocking capacity, reflecting and scattering UVB radiation [23]. Higher concentrations of nanosized TiO_2 form denser aggregates that establish a more effective barrier on the skin, reducing UV penetration [24]. Additionally, smaller TiO_2 particles exhibit greater photostability, further enhancing sunscreen efficacy. Coating and particle size were also shown to influence TiO_2 stability under UV exposure [22].

Effect of titanium dioxide and avobenzone

Fig. 2(b) illustrates the relationship between titanium dioxide (A) and avobenzone (C) with all other factors held constant. An increase in avobenzone led to a modest rise in SPF. This aligns with Beasley and Meyer [25], who reported that reducing avobenzone content up to 20% did not significantly impact SPF values in photostable formulations. As avobenzone mainly absorbs UVA, small changes in its concentration primarily affect UVA protection (PFA) rather than SPF, which is more influenced by UVB absorption. Moreover, avobenzone's photostability plays a role in overall sunscreen performance. However, the incorporation into an NLC system is not directly associated with improved photostability of avobenzone.

Puglia et al. [26] reported that avobenzone remained photolabile following incorporation into both NLCs and nanoemulsions, indicating that the protective effect of lipid-based carriers is dependent on the specific UV filter. In contrast, de Araújo et al. [27] demonstrated that an optimised combination of free and encapsulated NLC organic UV filters would improve the UVA and UVB photoprotection and simultaneously minimise the total concentration of UV filters. Therefore, the relatively modest contribution of avobenzone to the SPF response in the present study should not be interpreted as an absence of UVA protection. However, it reflects the limitation of using SPF as the sole optimisation response. Direct determination of UVA-PF, critical wavelength, and photostability would be required to establish the UVA and broad-spectrum performance of the developed formulation. Besides, studies have shown that its degradation under UV exposure can be minimised by adjusting solvent polarity, oil phase dielectric constant, and incorporating quenching agents [28,29]. These strategies help maintain its protective efficacy during sun exposure.

Effect of titanium dioxide and olive oil

Fig. 2(c) shows the interaction between titanium dioxide (A) and olive oil (D). Increasing olive oil concentration had a minimal effect on SPF, which remained in the range of 22–23. This is expected, as olive oil has a natural SPF of approximately 8 [30], and its photoprotective contribution is limited. Although higher concentrations of olive oil may slightly enhance SPF, its stability under UV exposure is not well-established [31]. Nevertheless, its antioxidant content, particularly tocopherol (10–20%), may provide additional skin protection by scavenging reactive oxygen species (ROS).

Model verification

To evaluate the model's accuracy, experimental and predicted SPF values from three randomly selected formulations were compared (**Table 6**). The experimental and predicted SPF values showed close agreement, with RSE values below 5%, supporting the predictive performance of the fitted model within the investigated design space.

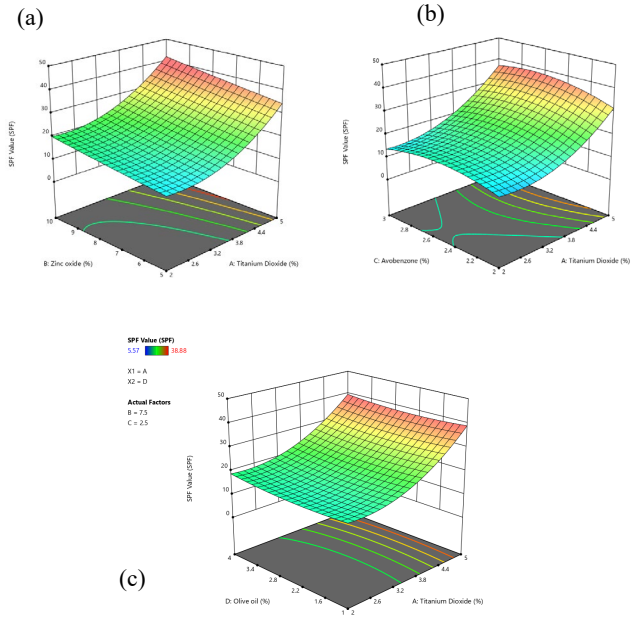

Fig. 2. Three-dimensional response surface plots showing the effects of formulation variables on SPF: (a) titanium dioxide and zinc oxide concentrations (avobenzone and olive oil held constant), (b) titanium dioxide and avobenzone concentrations (zinc oxide and olive oil held constant), and (c) titanium dioxide and olive oil concentrations (avobenzone and zinc oxide held constant).

Table 6. Validation sets of the model.

Independent Variables				SPF Value		Relative Standard Error (% RSE)
A (%)	B (%)	C (%)	D (%)	Experimental value	Predicted value	
4.8	9.6	2.0	1.6	31.99	33.03	3.16
4.6	9.4	2.2	1.4	32.90	33.31	1.23
3.8	9.2	2.4	2.2	26.37	25.32	4.15

Note: A: Titanium dioxide concentration, B: Zinc Oxide concentration- C: Avobenzone concentration- D: Olive oil concentration. All % are in (w/w) %.

Optimisation of NLC sunscreen formulation

Using the desirability function method in the Design-Expert® software, numerical optimisation was carried out. The optimised formulation was developed based on the value of all independent variables in the range, resulting in the maximum SPF values of the NLC formulation, as shown in **Table 7.**

Table 7. Constraints of numerical optimisation.

Variables	Goal	Lower Limit	Upper Limit
A	In range	2	5
B	In range	5	10
C	In range	2	3
D	In range	1	4
SPF Value	Maximize	5.57	38.88

Note; A: Titanium dioxide concentration, B: Zinc Oxide concentration- C: Avobenzone concentration- D: Olive oil concentration. All % are in (w/w) %.

Based on the D-Optimal-RSM, an optimised formulation with 5.00% (titanium dioxide), 8.00% (zinc oxide), 2.60% (Avobenzone) and 2.80% (Olive oil) was suggested, which would produce a SPF value of 39.09 and desirability of 1.00. The experimental SPF value of 38.88 showed close agreement with the predicted value, with an RSE of 0.54%, indicating that the model provided an acceptable prediction for the optimised formulation. **Table 8** shows the response values of the optimised Oleate NLC sunscreen formulation.

Table 8. Optimum formulation of the NLC formulation.

Independent Variables				SPF Value		Desirability	RSE (%)
A	B	C	D	Actual	Predicted		
5.0	8.0	2.6	2.8	38.88	39.09	1.00	0.54

Notre A: Titanium dioxide concentration, B: Zinc Oxide concentration- C: Avobenzone concentration- D: Olive oil concentration. All % are in (w/w) %.

Physicochemical characterisation of optimised NLC sunscreen formulation

Sun protection factor (SPF)

The optimised NLC formulation achieved an experimental SPF of 38.88, which closely matched the predicted value of 39.09. The relative standard error (RSE) was 0.54%, indicating strong agreement between experimental and modelled data. The formulation produced a high in vitro SPF value under the experimental conditions used. Sabzevari et al. reported that daily use of high-SPF sunscreens can improve skin texture and reduce pigmentation, highlighting the clinical benefits beyond UV protection [32].

Particle size and polydispersity index (PDI)

Table 9 shows the particle size and PDI of optimised NLC sunscreen formulation. The mean particle size was 170.10 nm, indicating the successful formation of a nanoscale dispersion. Particle sizes within this range have commonly been reported for NLC systems and may facilitate uniform distribution and surface coverage in topical formulations [2].

In the present study, the optimised formulation showed a PDI of 0.326, indicating a moderately narrow size distribution. Sahraee et al. stated that PDI with a value less than 0.3 indicates a good uniformity and colloidal stability [33]. Although this value was slightly above the ideal threshold, it remained acceptable for NLC-based topical formulations. The slight deviation may be due to high-shear homogenisation, partial aggregation of lipid particles, or differences in lipid–oil miscibility within the formulation system [34]. Furthermore, the reaction between the lipid and different oils may affect the distribution of the particles because they have complex fatty acid structures.

Table 9. Particle size and PDI of NLC formulation.

Property	
Particle size (nm)	170.10
PDI	0.326

pH of the formulation

The optimised formulation had a pH of 4.88, which is suitable for topical application as skin-compatible formulations are generally recommended to fall within the mildly acidic range of approximately pH 4–6 [35]. This value is consistent with the natural acidic environment of healthy human skin. The slightly acidic pH of the NLC sunscreen formulation may reflect the combined influence of the aqueous phase and other formulation components rather than a single ingredient. A mildly acidic pH has similarly been reported in olive-oil-containing topical emulsions [36].

Spreadability

Spreadability is a key performance parameter for topical systems, especially for inflamed or sensitive skin, because it influences application comfort and uniform film formation. The NLC showed a spread diameter of 3.22 cm and a spreadability of 5.4 $g \cdot cm \cdot s^{-1}$. As reported by Al-Sarraf et al., larger diameters generally reflect better spreadability and improved skin coverage

with reduced drag [37]. These findings are comparable to those of Abdel-Salam et al. for NLC-based sunscreens [22]. Overall, the favourable spreading behaviour suggests an appropriate consistency for forming an even film on the skin surface. **Fig. 3** presents the formulation before and after brass weight was applied, respectively.

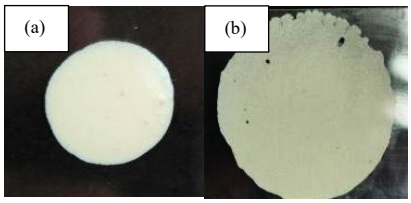

Fig. 3. NLC formulation on a glass tile (a) before and (b) after application of the brass weight.

Stability study

A) Centrifugation test

The optimised NLC formulation demonstrated good physical stability, with no visible phase separation observed after centrifugation at 4000 rpm for 15 minutes. This suggests a uniform dispersion and consistent density between the formulation components.

B) Freeze-thaw cycle

After three freeze–thaw cycles (−18 °C/40 °C over three days), the formulation showed no phase separation, or change in appearance was observed, indicating preservation of macroscopic homogeneity. However, the mean particle size increased from 170.10 nm to 290.7 nm but remained nanoscale while the PDI increased to 0.378. The increase in particle size and PDI suggests partial particle aggregation and reduced homogeneity following freeze–thaw stress [23]. Therefore, the formulation should not be considered fully stable based on visual appearance alone. Further optimisation of the interfacial stabilisation system and confirmation through long-term and accelerated stability studies are required.

Tyrosinase inhibition activity

Tyrosinase is a key enzyme involved in melanogenesis, and excessive tyrosinase activity is associated with pigmentary disorders such as hyperpigmentation and melasma and has also been implicated in melanoma biology [38]. The inhibitory effects of free KMO and KMO-containing NLCs on mushroom tyrosinase were evaluated using L-tyrosine as the substrate, with kojic acid included as the positive control. As shown in **Fig. 4**, all tested samples exhibited increasing tyrosinase inhibition with increasing concentration. Two-way ANOVA demonstrated significant effects of formulation type, $F(2, 42) = 1701.92$, $p < 0.0001$, and concentration, $F(6, 42) = 536.72$, $p < 0.0001$, on tyrosinase-inhibitory activity. A significant formulation–concentration interaction was also observed, $F(12, 42) = 12.94$, $p < 0.0001$, indicating that the effect of formulation type varied across the tested concentrations.

Tukey's multiple-comparisons test showed that the KMO-containing NLC formulation produced significantly greater inhibition than free KMO at all concentrations tested ($p < 0.05$). From 5 to 250 µg/mL, the NLC formulation also exhibited significantly higher inhibitory activity than kojic acid ($p < 0.05$). At 500 µg/mL, however, no significant difference was observed between the NLC formulation and kojic acid ($p = 0.94$). At 250 µg/mL, the KMO-containing NLC formulation produced 78.08% inhibition, compared with 62.30% for free KMO and 73.03% for kojic acid. These findings suggest that incorporation of KMO into the NLC-based formulation improved its apparent tyrosinase-inhibitory performance under the assay conditions. This enhancement may be related to improved dispersion or availability of KMO in the aqueous assay medium. However, the underlying mechanism was not directly investigated. Similar enhancement of tyrosinase inhibition following nanoformulation of KMO has been reported by Roselan et al. [20]. KMO has also been reported to possess antioxidant activity, which may provide additional functional value in topical cosmeceutical formulations by reducing oxidative stress [13,39].

Nevertheless, the present results demonstrate only inhibition of mushroom tyrosinase in a cell-free enzyme assay. They do not confirm reduced intracellular melanogenesis or clinical depigmenting efficacy. Further studies using human melanocytes or B16F10 cells, including measurements of intracellular tyrosinase activity and melanin content, are required to determine whether the observed enzyme inhibition translates into a cellular depigmenting effect.

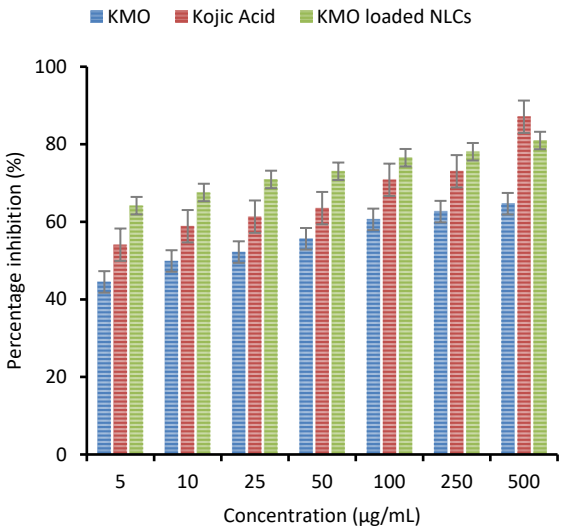

Fig. 4. Tyrosinase inhibitory activity of free KMO, KMO-loaded NLC and kojic acid against mushroom tyrosinase at different concentrations. Data are presented as mean ± SD (n = 3). Statistical analysis was performed using two-way ANOVA followed by Tukey's multiple comparisons test.

Scientific implications, limitations and future perspectives

The present study provides preliminary evidence supporting the potential of the optimised KMO-containing NLC sunscreen formulation as a multifunctional sunscreen by combining high in vitro SPF with tyrosinase-inhibitory activity. However, several limitations should be acknowledged. UVA protection factor (UVA-PF), critical wavelength, photostability, and water-resistance performance were not evaluated. As SPF predominantly represents protection against UVB-induced erythema, the measured SPF value alone should not be interpreted as evidence of UVA or broad-spectrum photoprotection. Furthermore, zeta potential, encapsulation efficiency, drug loading, and particle morphology were not determined, limiting the interpretation of colloidal stability, KMO incorporation, and nanoparticle structure. The tyrosinase-inhibition findings were obtained using a cell-free mushroom tyrosinase assay and therefore do not confirm inhibition of intracellular melanogenesis or clinical depigmenting efficacy.

Precise IC_{50} values were also not determined because the selected concentration range did not adequately encompass the 50% inhibition response for all samples. Cytotoxicity, dermal irritation, phototoxicity, skin permeation and retention, and long-term storage stability were also not assessed.

Future studies should determine UVA-PF and critical wavelength using a recognised standardised method, such as ISO 24443:2021, and evaluate photostability following controlled UV exposure and water-resistance performance. Comprehensive physicochemical characterisation of the NLC system should also be performed to clarify its colloidal properties and the incorporation of KMO. Skin permeation and retention should be investigated using appropriate ex vivo skin models. Safety evaluation should include cytotoxicity, reconstructed human epidermis irritation testing according to OECD Test Guideline 439 [40], and appropriate phototoxicity testing according to OECD Test Guideline 432 [41]. The observed tyrosinase-inhibitory activity should also be confirmed using human melanocytes or B16F10 cells through measurements of intracellular tyrosinase activity and melanin content. Long-term and accelerated stability studies under applicable ICH-aligned conditions, together with comparison against a suitable commercial sunscreen, would further establish the formulation's stability, safety, and relative performance.

CONCLUSION

A nanostructured lipid carrier (NLC)-based sunscreen was successfully developed and optimised using bath ultrasonication followed by high-shear homogenisation. The formulation, containing kojic monooleate (KMO), titanium dioxide, zinc oxide, avobenzone, and olive oil, was optimised via Response Surface Methodology (RSM). Titanium dioxide, zinc oxide, and avobenzone were identified as significant contributors to SPF, while olive oil had a minimal effect. The optimised formulation achieved a predicted SPF of 39.09 and an experimental SPF of 38.88. It demonstrated desirable physicochemical properties, including a particle size of 170.10 nm, a PDI of 0.326, and a pH of 4.88 indicating compatibility for topical application. No macroscopic phase separation was observed following centrifugation, whereas freeze–thaw cycling increased particle size and PDI, indicating reduced colloidal stability under thermal stress. Further improvement of colloidal and long-term stability is necessary. These results highlight the potential of KMO-loaded NLC as an SPF-oriented sunscreen platform with added cosmeceutical benefits.

CONFLICT OF INTEREST

The authors declare no conflict of interest.

FUNDING STATEMENT

The authors declare that they have received no funding for this research.

DATA AVAILABILITY STATEMENT

All data supporting the findings of this study are included within the manuscript.

SUPPLEMENTARY DATA

Not applicable.

ACKNOWLEDGEMENT

The authors gratefully acknowledge Laboratory 120, Block D, Faculty of Science, Universiti Putra Malaysia, and the Bioprocessing and Biomanufacturing Research Centre, Universiti Putra Malaysia for providing the laboratory facilities and technical support required to conduct this research.

REFERENCES

1. Gaikwad S, Kasture A. Nanostructured lipid carriers in cosmeceuticals. Int J Creat Res Thoughts. 2024;12(5):317–322.
2. Javed S, Mangla B, Almoshari Y, Sultan MH, Ahsan W. Nanostructured lipid carrier system: a compendium of their formulation development approaches, optimization strategies by quality by design, and recent applications in drug delivery. Nanotechnol Rev. 2022;11(1):1744–1777. https://doi.org/10.1515/ntrev-2022-0109
3. Meticulous Research. Sunscreen market by product type, SPF range, form, distribution channel, end user and geography global forecast to 2035. 2025 (cited 2026 Jul 23). Available from: https://www.meticulousresearch.com/product/sunscreen-market-6173
4. Salvi VR, Pawar P. Nanostructured lipid carriers (NLC) system: a novel drug targeting carrier. J Drug Deliv Sci Technol. 2019;51:255–267. https://doi.org/10.1016/j.jddst.2019.02.017
5. Ghasemiyeh P, Mohammadi-Samani S. Solid lipid nanoparticles and nanostructured lipid carriers as novel drug delivery systems: applications, advantages and disadvantages. Res Pharm Sci. 2018;13(4):288–303. https://doi.org/10.4103/1735-5362.235156
6. Chu CC, Hasan ZAA, Tan CP, Nyam KL. In vitro safety evaluation of sunscreen formulation from nanostructured lipid carriers using human cells and skin model. Toxicol In Vitro. 2022;84:105431. https://doi.org/10.1016/j.tiv.2022.105431
7. Therapeutic Goods Administration. Literature review on the safety of titanium dioxide and zinc oxide nanoparticles in sunscreens (Internet). Canberra: Australian Government Department of Health; 2017 Available from: https://www.tga.gov.au/resources/publication/corporate-reports/literature-review-safety-titanium-dioxide-and-zinc-oxide-nanoparticles-sunscreens
8. Syed Azhar SNF, Ashari SE, Salim N. Development of a kojic monooleate-enriched oil-in-water nanoemulsion as a potential carrier for hyperpigmentation treatment. Int J Nanomedicine. 2018;13:6465–6479. https://doi.org/10.2147/IJN.S171532
9. Lajis AFB, Hamid M, Ariff AB. Depigmenting effect of kojic acid esters in hyperpigmented B16F1 melanoma cells. J Biomed Biotechnol. 2012;2012:952452. https://doi.org/10.1155/2012/952452
10. Subramaniam B, Siddik ZH, Nagoor NH. Optimisation of nanostructured lipid carriers: understanding the types, designs, and parameters in the process of formulations. J Nanopart Res. 2020;22(6):141. https://doi.org/10.1007/s11051-020-04848-0
11. International Organization for Standardization. ISO 24443:2021 Cosmetics—Determination of sunscreen UVA photoprotection in vitro (Internet). 2nd ed. Geneva: International Organization for Standardization; 2021 (cited 2026 Jul 23). Available from: https://www.iso.org/standard/75059.html
12. U.S. Food and Drug Administration. Labeling and effectiveness testing: sunscreen drug products for over-the-counter human use—small entity compliance guide (Internet). Silver Spring (MD): U.S. Food and Drug Administration; 2012 (cited 2026 Jul 23). Available from: https://www.fda.gov/regulatory-information/search-fda-guidance-documents/labeling-and-effectiveness-testing-sunscreen-drug-products-over-counter-human-use-small-entity
13. Jumbri K, Rozy MFA, Ashari SE, Mohamad R, Basri M, Masoumi HRF. Optimisation and characterisation of lipase-catalysed synthesis of a kojic monooleate ester in a solvent-free system by response surface methodology. PLoS One. 2015;10(12):e0144664. https://doi.org/10.1371/journal.pone.0144664
14. International Organization for Standardization. ISO 22412:2025 Particle size analysis—Dynamic light scattering (DLS). 3rd ed. Geneva: International Organization for Standardization; 2025. https://www.iso.org/standard/85505.html

15. Stetefeld J, McKenna SA, Patel TR. Dynamic light scattering: a practical guide and applications in biomedical sciences. Biophys Rev. 2016;8(4):409–427. https://doi.org/10.1007/s12551-016-0218-6
16. Hou P, Pu F, Zou H, Diao M, Zhao C, Xi C, et al. Whey protein-stabilized nanoemulsion: a potential delivery system for ginsenoside Rg3. Food Biosci. 2019;31:100427. https://doi.org/10.1016/j.fbio.2019.100427
17. Garg A, Aggarwal D, Garg S, Singla AK. Spreading of semisolid formulations: an update. Pharm Technol. 2002;26(9):84–105.
18. Varma VNSK, Maheshwari PV, Navya M, Reddy SC, Shivakumar HG, Gowda DV. Calcipotriol delivery into the skin as emulgel for effective permeation. Saudi Pharm J. 2014;22(6):591–599. https://doi.org/10.1016/j.jsps.2014.02.007
19. Qian Y, Qiu X, Zhu S. Sunscreen performance of lignin from different technical resources and their general synergistic effect with synthetic sunscreens. ACS Sustain Chem Eng. 2016;4(7):4029–4035. https://doi.org/10.1021/acssuschemeng.6b00934
20. Roselan MA, Zakaria N, Faujan NH, Mohammad Latif MA, Mohd Faudzi SM, Ab Hadi H, et al. In vitro cytotoxicity assay, mushroom tyrosinase inhibitory activity and release analysis of kojic monooleate nanodelivery system and in silico molecular docking study against 2Y9X target enzyme. J Drug Deliv Sci Technol. 2021;66:102764. https://doi.org/10.1016/j.jddst.2021.102764
21. Ghamarpoor R, Fallah A, Jamshidi M. Investigating the use of titanium dioxide (TiO_2) nanoparticles on the amount of protection against UV irradiation. Sci Rep. 2023;13(1):9793. https://doi.org/10.1038/s41598-023-37057-5
22. Abdel-Salam FS, Ammar HO, Elkheshen SA, Mahmoud AA. Anti-inflammatory sunscreen nanostructured lipid carrier formulations. J Drug Deliv Sci Technol. 2017;37:13–19. https://doi.org/10.1016/j.jddst.2016.10.014
23. Date PV, Samad A, Devarajan PV. Freeze thaw: a simple approach for prediction of optimal cryoprotectant for freeze drying. AAPS PharmSciTech. 2010;11(1):304–313. https://doi.org/10.1208/s12249-010-9382-3
24. Lin CC, Lin WJ. Sun protection factor analysis of sunscreens containing titanium dioxide nanoparticles. J Food Drug Anal. 2011;19(1):1–8. https://doi.org/10.38212/2224-6614.2181
25. Beasley DG, Meyer TA. Characterization of the UVA protection provided by avobenzone, zinc oxide, and titanium dioxide in broad-spectrum sunscreen products. Am J Clin Dermatol. 2010;11(6):413–421. https://doi.org/10.2165/11537050-000000000-00000
26. Puglia C, Damiani E, Offerta A, Rizza L, Tirendi GG, Tarico MS, et al. Evaluation of nanostructured lipid carriers and nanoemulsions as carriers for UV filters: characterization, in vitro penetration and photostability studies. Eur J Pharm Sci. 2014;51:211–217. https://doi.org/10.1016/j.ejps.2013.09.023
27. de Araújo MM, Schneid AC, Oliveira MS, Mussi SV, de Freitas MN, Carvalho FC, et al. NLC-based sunscreen formulations with optimized proportion of encapsulated and free filters exhibit enhanced UVA and UVB photoprotection. Pharmaceutics. 2024;16(3):427. https://doi.org/10.3390/pharmaceutics16030427
28. Nash JF, Tanner PR. Relevance of UV filter/sunscreen product photostability to human safety. Photodermatol Photoimmunol Photomed. 2014;30(2–3):88–95. https://doi.org/10.1111/phpp.12113
29. Bonda CA. The photostability of organic sunscreen actives: a review. In: Shaath NA, editor. Sunscreens: regulations and commercial development. 3rd ed. Boca Raton (FL): CRC Press; 2005. p. 321–349. https://doi.org/10.1201/b14170-25
30. Kaur CD, Saraf S. In vitro sun protection factor determination of herbal oils used in cosmetics. Pharmacogn Res. 2010;2(1):22–25. https://doi.org/10.4103/0974-8490.60586
31. Rahmasari D, Putri NS, Pranita EN, Nadifa N, Anggraeni AD. Development of emulsion gel sunscreen containing olive oil and clove oil. KnE Med. 2022;2(3):141–148. https://doi.org/10.18502/kme.v2i3.11862
32. Sabzevari N, Qiblawi SH, Norton SA, Fivenson DP. Sunscreens: UV filters to protect us. Part 1: changing regulations and choices for optimal sun protection. Int J Womens Dermatol. 2021;7(1):28–44. https://doi.org/10.1016/j.ijwd.2020.05.017
33. Sahraee S, Ghanbarzadeh B, Mohammadi M, Pezeshki A, Hoseini M. Development of heat-stable gelatin-coated nanostructured lipid carriers: colloidal and stability properties. LWT. 2022;160:113265. https://doi.org/10.1016/j.lwt.2022.113265
34. Khosa A, Reddi S, Saha RN. Nanostructured lipid carriers for site-specific drug delivery. Biomed Pharmacother. 2018;103:598–613. https://doi.org/10.1016/j.biopha.2018.04.055
35. Lukić M, Pantelić I, Savić SD. Towards optimal pH of the skin and topical formulations: from the current state of the art to tailored products. Cosmetics. 2021;8(3):69. https://doi.org/10.3390/cosmetics8030069
36. Smaoui S, Ben Hlima H, Jarraya R, Kamoun NG, Ellouze R, Damak M. Cosmetic emulsion from virgin olive oil: formulation and bio-physical evaluation. Afr J Biotechnol. 2012;11(40):9664–9671. https://doi.org/10.5897/AJB12.163
37. Al-Sarraf MA, Hussein AA, Al-Sarraf ZA. Comparison between conventional gel and nanostructured lipid carrier gel of zaltoprofen: preparation and in vitro/ex vivo evaluation. Int J Drug Deliv Technol. 2021;11(3):988–995. https://doi.org/10.25258/ijddt.11.3.57
38. Chatatikun M, Tedasen A, Pattaranggoon NC, Palachum W, Chuaijit S, Mudpan A, et al. Antioxidant activity, anti-tyrosinase activity, molecular docking studies, and molecular dynamic simulation of active compounds found in nipa palm vinegar. PeerJ. 2023;11:e16494. https://doi.org/10.7717/peerj.16494
39. Jaslina NF, Ashari SE, Mohamad R, Faujan NH. In vitro and antioxidant evaluation of a nanoemulsion formulation containing kojic monooleate for hyperpigmentation treatment. Malays J Chem. 2021;23(4):37–48. https://doi.org/10.55373/mjchem.v23i4.1185
40. Organisation for Economic Co-operation and Development. Test No. 439: In vitro skin irritation: reconstructed human epidermis test method. OECD Guidelines for the Testing of Chemicals, Section 4. Paris: OECD Publishing; 2025. https://doi.org/10.1787/9789264242845-en
41. Organisation for Economic Co-operation and Development. Test No. 432: In vitro 3T3 NRU phototoxicity test. OECD Guidelines for the Testing of Chemicals, Section 4. Paris: OECD Publishing; 2019. https://doi.org/10.1787/9789264071162-en